Trend-extracted MSE Based on Adaptive Aligned EEMD with Early Termination Scheme

Analysis of the Acute Stroke Patients' Physiological Signals

Pei-Wen Huang[1], Wei-Jung Jou[1], Yu-Min Lin[1], Hsiao-I Jen[1], Sung-Chun Tang[2], Dar-Ming Lai[3], An-Yeu (Andy) Wu[1]
[1]Graduate Institute of Electronics Engineering, National Taiwan University, Taipei, Taiwan
[2]Stroke Center and Department of Neurology, National Taiwan University Hospital, Taipei, Taiwan
[3]Division of Neurosurgery, Department of Surgery, National Taiwan University Hospital, Taipei, Taiwan
[1]{pwhuang, middle, yumin, hsiaoi, andywu}@access.ee.ntu.edu.tw, [2]tangneuro@gmail.com, [3]002867@ntuh.gov.tw

***Abstract*—Multiscale entropy (MSE) analysis method has been widely used to evaluate the physiologic control mechanisms. However, MSE is vulnerable to trends. Ensemble empirical mode decomposition (EEMD) is a powerful tool to remove the trend from non-stationary physiological signals before MSE analysis. In this paper, trend-extracted MSE (T-MSE) based on adaptive aligned EEMD (AA-EEMD) with early termination scheme is proposed. AA-EEMD not only reduces the computing time, but also considers the frequency meaning of different physiological signals and different subjects. We have applied T-MSE based on AA-EEMD to analyze the acute stroke patients' physiological signals in intensive care unit (ICU). We find that the complexity of electrocardiogram (EKG) is higher in the acute stroke patients with good functional outcome than those with bad functional outcome. For EKG parameter, the p-value is approximately 10^{-8}, which shows significant statistical difference. Moreover, the average number of IMFs in a single member of ensemble is reduced to 74% of the original. The average computing time in a single member of ensemble is reduced to 76%. Also, the average computing time of combining EEMD and MSE is reduced to 72%.**

Keywords—early termination, multiscale entropy, ensemble empirical mode decomposition, intrinsic mode functions, physiological signal, acute stroke

I. INTRODUCTION

Multiscale entropy (MSE) analysis method has been widely used to evaluate the physiologic control mechanisms, including heart failure [1], atrial fibrillation [1], Alzheimer's disease [2], type I diabetes mellitus [3] and traumatic brain injury [4]. Wide classes of disease degrade the physiologic information in physiological signals. Therefore, decreasing of complexity is a generic feature of pathologic dynamics [5]. In contrast, healthy systems exhibit meaningful and complex control mechanisms. Thus, high entropy values appear at multiple scales [1].

Compared with traditional single scale entropy and single scale variability, MSE can analyze the complexity and variability of a signal from small scales to large scales [6]. Thus, applying MSE to analyze physiological signals can interpret the short-term and long-term regulations. However, the measured signal, $\hat{S}_{measure}(t)$ consists of not only the physiological signal, $S_{physiology}(t)$ coming from the subject but also the additional "trend", $S_{trend}(t)$ caused by the background signal. It can be formulated as

This work has been supported by: National Taiwan University (NTU)-National Taiwan University Hospital (NTUH)-MediaTek Innovative Medical Electronics Research Center, NTUH PC851.

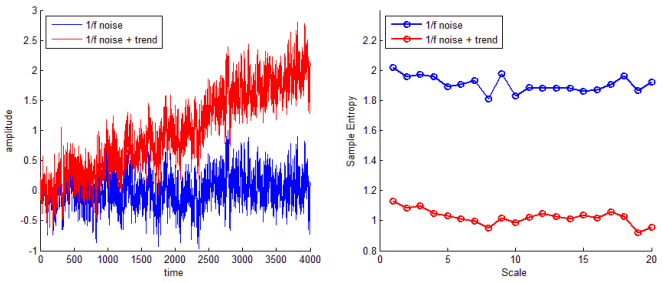

(a) (b)

Fig. 1. (a) Time domain signal. (b) MSE analysis result. After adding an additional trend to 1/f noise, *SampEn* on each scale decreases.

$$\hat{S}_{measure}(t) = S_{physiology}(t) + S_{trend}(t). \quad (1)$$

After adding an additional trend to 1/f noise, *SampEn* on each scale decreases, as shown in Fig.1. $S_{trend}(t)$ reveals the tendency or direction of a signal. Due to the existence of $S_{trend}(t)$, the complexity of $S_{physiology}(t)$ is underestimated. Therefore, "de-trend" is a necessary process before applying MSE. We remove the estimated trend, $\hat{S}_{trend}(t)$ from $\hat{S}_{measure}(t)$, and get the estimated physiological signal, $\hat{S}_{physiology}(t)$. It can be formulated as

$$\hat{S}_{physiology}(t) = \hat{S}_{measure}(t) - \hat{S}_{trend}(t). \quad (2)$$

Polynomial fitting or high pass filter cannot completely remove the non-stationary trends [2]. In contrast, EMD decomposes non-stationary physiological signals into *M* intrinsic mode functions (IMFs), each of which represents an oscillation mode. The comparison of high pass filter and EMD is shown in Fig. 2. EMD suffers from a mode-mixing problem. That is, an IMF contains different oscillation modes or one mode in different IMFs [10]. Ensemble EMD (EEMD) is proposed by [7] to solve the mode-mixing problem in EMD.

However, the calculation of EEMD contains *N* EMD. Because *N* is large, normally up to 100, it is quite time-consuming. To reduce the computing time, combining EEMD and MSE properly is necessary. In addition, there are two design issues. First, different types of physiological signals define their physiological meanings in different ways. Second, we should note that some of the $\hat{S}_{measure}(t)$ contain larger

proportion of $\hat{S}_{trend}(t)$ than the others. Thus, the way of selecting IMFs to represent $\hat{S}_{physiology}(t)$ should also be considered. It is improper that [8] selects a fixed amount of IMFs for all the subjects. Therefore, we propose trend-extracted MSE (T-MSE) based on adaptive aligned EEMD (AA-EEMD) with early termination scheme, which is able to reduce the computing time and consider the frequency meaning of different physiological signals and different subjects.

The rest of the paper is organized as follows: Section II introduces MSE, EMD and EEMD. Section III presents the proposed T-MSE based on AA-EEMD with early termination scheme. Section IV presents the experimental data and result. Section V is the conclusion.

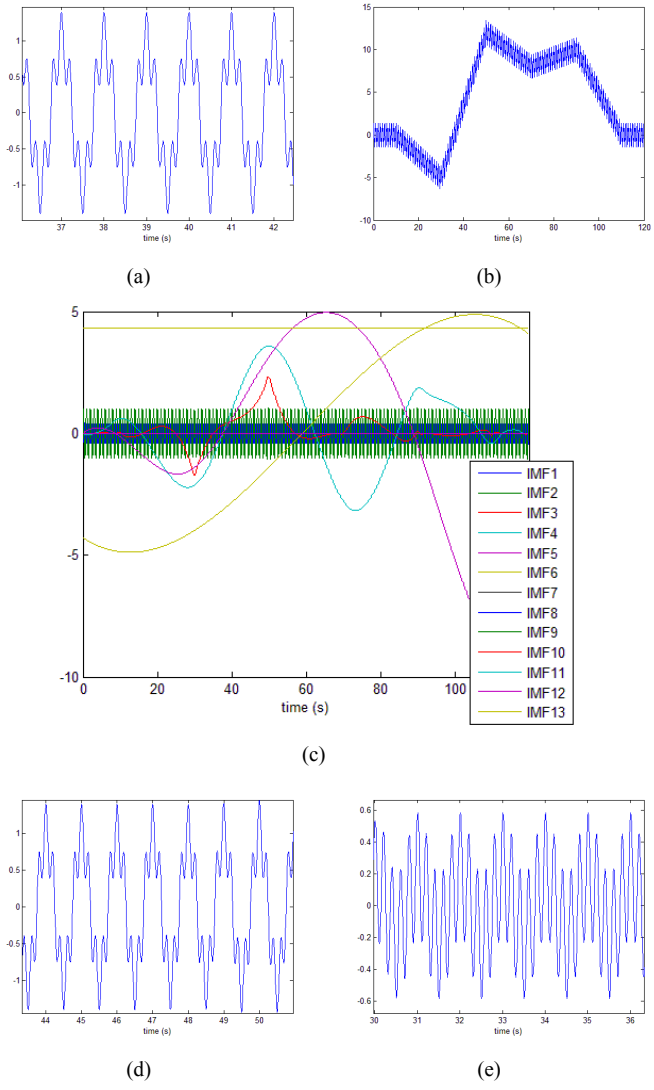

(a) (b) (c) (d) (e)

Fig. 2. Assume x is the signal we desire, $x = cos(2\pi f_1 t) + 0.4\,cos(2\pi f_2 t)$, where $f_1 = 1$ Hz and $f_2 = 5$ Hz. x is shown in Fig. 2(a). A non-stationary trend is generated and added to x, $y = x + trend$, as shown in Fig. 2(b). We use EMD for de-trending y. The result of EMD is shown in Fig. 2(c). We can find that IMF1 and IMF2 are components of x. Others are caused by $trend$. It is simply choose the top 2 IMF in Fig. 2(c) to recover x, as shown in Fig. 2(d). As a comparison, we apply a high pass filter which has cut-off frequency $(1-\delta)$ Hz (just a little below f_1) to de-trend y. The de-trended result is shown in Fig. 2(e). It is not difficult to find that in Fig. 2(e), we cannot completely remove non-stationary trend and recover x.

II. Background

A. Multiscale Entropy (MSE) [1-6]

MSE analyzes the signal complexity in the perspective of different scales. There are two steps in MSE analysis. First, calculate multiple coarse-grained time series:

$$y_j^\tau = \frac{1}{\tau}\sum_{i=(j-1)\tau+1}^{j\tau} x_i, 1 \le i \le N, 1 \le j \le \frac{N}{\tau} \quad (3)$$

where x_i is the time series of input, N is the length of the input time series, and τ is the scale factor. Second, calculate the sample entropy (*SampEn*) for each y_j^τ:

$$SampEn(y_j^\tau, m, r) = -\ln\left[\frac{B^{m+1}(r)}{B^m(r)}\right], \quad (4)$$

where m is the pattern length and r is the similarity criterion. The probability $B^m(r)$ or $B^{m+1}(r)$ measures whether the distance between two vectors is lower than r in m-dimensional space or (m+1)-dimensional space. Due to the existence of $S_{trend}(t)$, the standard deviation of $\hat{S}_{measure}(t)$ becomes larger than $S_{physiology}(t)$. Similarity criterion r is in proportion to standard deviation. Larger r results in more matching patterns and thus lower complexity.

B. Empirical Mode Decomposition (EMD)

EMD is suitable to decompose non-stationary physiological signals [2,7-8]. EMD uses the shifting process to iteratively decompose the input signal $x(t)$. The algorithm of EMD is illustrated as follows [9-10]. First, initialize $x'(t)$ as $x(t)$. Second, find the location of all the maxima and minima of $x'(t)$. Third, interpolate between all the maxima (cf. minima) to get the upper (cf. lower) envelopes, e_{max} (cf. e_{min}). Fourth, shift means of upper and lower envelopes:

$$d(t) = x'(t) - (e_{max} + e_{min}) * 0.5\,. \quad (5)$$

Then, check whether $d(t)$ satisfies the criterion of IMF. There are two criteria of IMF: The number of extremes and the number of zero-crossings must either equal or differ at most by one; at any point, the mean value of e_{max} and e_{min} is near to zero. If $d(t)$ does not satisfy the criterion of IMF, set

$$x'(t) = d(t) \quad (6)$$

and go to the first step. Otherwise, set

$$IMF_m(t) = d(t), x'(t) = x'(t) - IMF_m(t) \quad (7)$$

and check whether the number of extrema of $x'(t)$ is less than two. If not, go to the first step. Otherwise, stop the shift process. After EMD, the input signal is decomposed into M IMFs and a residual:

$$x(t) = \sum_{m=1}^{m=M} IMF_m(t) + residual(t). \quad (8)$$

C. Ensemble Empirical Mode Decomposition (EEMD)

EMD suffers from mode-mixing, which obscures the physiological meaning of IMFs. EEMD is proposed to solve

the mode-mixing problem in EMD. The algorithm of EEMD is illustrated as follows [9-10]. First, generate the ensemble $s_n(t)$:

$$s_n(t) = x(t) + w_n(t), 1 \le n \le N \quad (9)$$

where $x(t)$ is the original signal, $w_n(t) \sim \mathcal{N}(0, \sigma^2)$ is additive white Gaussian noise (AWGN), and N is the ensemble number. Second, decompose each $s_n(t)$ into $IMF_m^n(t)$ using EMD:

$$s_n(t) = IMF_m^n(t), 1 \le n \le N, 1 \le m \le M \quad (10)$$

where $IMF_m^n(t)$ represents the mth IMF of the nth member of ensemble. Finally, average the IMFs with the same index across the ensemble. For example, the mth IMF of EEMD output is obtained as

$$\overline{IMF}_m = \left(\frac{1}{N}\right) \sum_{n=1}^{N} IMF_m^n(t). \quad (11)$$

III. Proposed Trend-Extracted MSE (T-MSE) Based on Adaptive Aligned EEMD (AA-EEMD) with Early Termination Scheme

The block diagram of the proposed T-MSE based on AA-EEMD with early termination scheme is shown in Fig. 3. There are three blocks: MSE, EEMD, and the control block. The control block checks criteria. Checking criteria avoids the redundant computation, and thus reduces the computing time. The input and output of the control block is illustrated as follows:

1) $IMF_m^n(t)$: $IMF_m^n(t)$ is the output of EEMD in the mth shifting process of nth member of ensemble.
2) f_{thr}: f_{thr} is a threshold defined in frequency domain. The frequency higher than f_{thr} is regarded as $\hat{S}_{physiology}(t)$. In contrast, the frequency lower than f_{thr} is regarded as $\hat{S}_{trend}(t)$.
3) TER_{EEMD}: TER_{EEMD} is the termination signal of EEMD. Only when TER_{EEMD} equals to 1, the EEMD will be terminated early. Otherwise, it will not.

A. *Early Termination*

For an input signal $\hat{S}_{measure}(t)$, EEMD will decompose it into M IMFs and a residual

$$\hat{S}_{measure}(t) = \sum_{m=1}^{m=M} \overline{IMF}_m(t) + residual(t). \quad (12)$$

Each IMF represents an oscillatory mode. In our design, EEMD is only applied to remove the non-stationary trends $\hat{S}_{trend}(t)$ from $\hat{S}_{measure}(t)$. Instead of M IMFs, we only need K IMFs to represent our estimated physiological signals $\hat{S}_{physiology}(t)$

$$\hat{S}_{measure}(t) = \sum_{m=1}^{m=K} \overline{IMF}_m(t) + \hat{S}_{trend}(t). \quad (13)$$

Compare (12) with (13). It is obvious that the computing of $\overline{IMF}_{K+1}(t), \overline{IMF}_{K+2}(t), \dots, \overline{IMF}_M(t)$ is redundant and time-consuming. The steps of T-MSE based on AA-EEMD with early termination scheme are illustrated as follows:

Step 1: Set f_{thr} and input $\hat{S}_{measure}(t)$ into EEMD.

Step 2: Generate the ensemble

$$s_n(t) = \hat{S}_{measure}(t) + w_n(t), 1 \le n \le N \quad (14)$$

where $w_n(t) \sim \mathcal{N}(0, \sigma^2)$ is AWGN; N is the ensemble number. In this paper, we set $\sigma = 0.2$ and $N = 100$.

Step 3: Decompose every member of the ensemble $s_n(t)$ by using AA-EEMD: First, generate an $IMF_m^n(t)$ by using shift process and send the $IMF_m^n(t)$ to the control block. Second, the control block conducts fast Fourier transform (FFT) to transfer $IMF_m^n(t)$ into frequency domain:

$$X_{IMF}(k) = \sum_{j=1}^{N} IMF_m^n(j) \omega_N^{(j-1)(k-1)} \quad (15)$$

where $\omega_N = e^{(-2\pi i)/N}$. Calculate the percentage of frequency components below f_{thr}:

$$\frac{\sum_{k=1}^{\frac{f_{thr}}{f_s} * N} X_{IMF}(k)}{\sum_{k=1}^{N} X_{IMF}(k)} \quad (16)$$

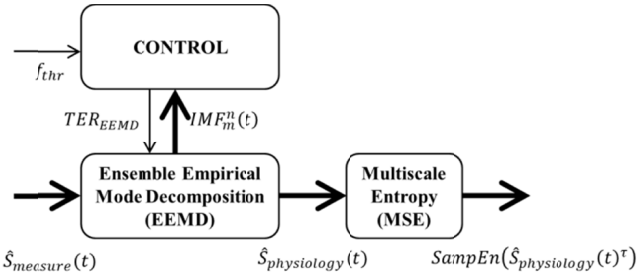

Fig. 3. The block diagram of T-MSE based on AA-EEMD with early termination scheme.

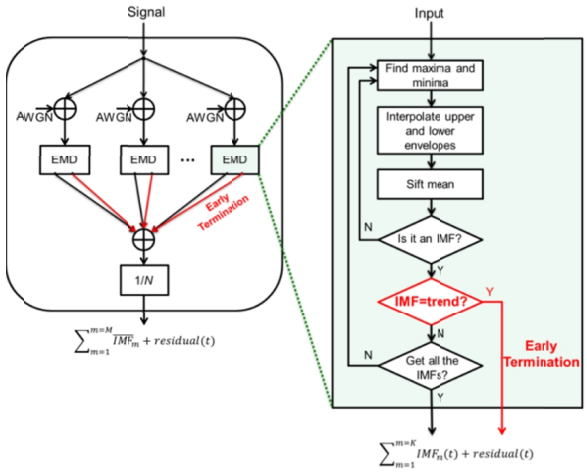

Fig. 4. The flow chart of AA-EEMD.

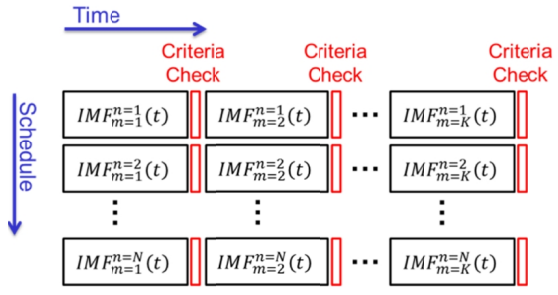

Fig. 5. The timing diagram of AA-EEMD.

where f_s is the sampling frequency. If the percentage is less than 50%, $IMF_m^n(t)$ will be taken as a component of $\hat{S}_{physiology}(t)$. Set TER_{EEMD} to 0. That is, EMD will not be terminated early. In contrast, if the percentage is not less than 50%, $IMF_m^n(t)$ will be taken as a component of $\hat{S}_{trend}(t)$. Set TER_{EEMD} to 1. That is, EMD will be terminated early. Assume the number of generated IMFs to be K. Then, $s_n(t)$ can be expressed as

$$s_n(t) = IMF_m^n(t), 1 \le n \le N, 1 \le m \le K. \quad (17)$$

Step 4: Average IMFs with the same index across the ensemble:

$$\overline{IMF}_m = \left(\frac{1}{N}\right) \sum_{n=1}^{N} IMF_m^n(t), 1 \le m \le K. \quad (18)$$

Step 5: Sum all of the IMFs (K IMFs) to represent $\hat{S}_{physiology}(t)$:

$$\hat{S}_{physiology}(t) = \sum_{m=1}^{m=K} \overline{IMF}_m(t). \quad (19)$$

Step 6: Apply MSE to analyze $\hat{S}_{physiology}(t)$, which reflects the physiologic control mechanisms.

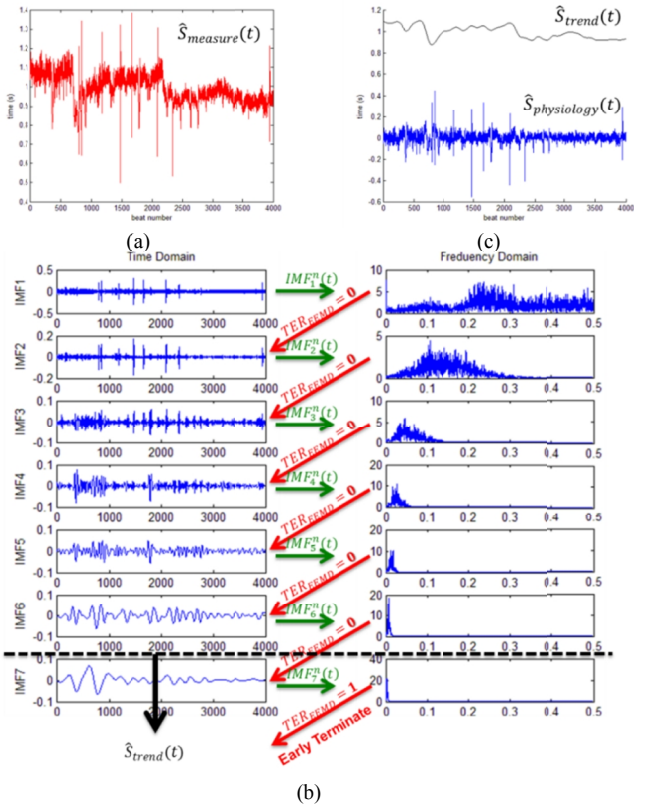

Fig. 6. (a) $\hat{S}_{measure}(t)$. (b) Left: IMF in time domain. Right: IMF in frequency domain. The original signal is decomposed into 6 IMFs and a trend. (c) The blue line is the summation of the 6 IMFs, which relates to $\hat{S}_{physiology}(t)$, whereas the black line is $\hat{S}_{trend}(t)$.

TABLE I. SUMMARY OF DATA COLLECTION.

Signal	Number of patients		
	mRS 0-2	mRS 3-6	Total
EKG	64	86	150

The flow chart of AA-EEMD is shown in Fig. 4. Checking criteria "IMF=trend?" avoids the redundant computation, and thus reduces the computing time. The timing diagram of AA-EEMD is shown in Fig. 5. Criteria are attached after each shifting processing. For every member of the ensemble $s_n(t)$, EMD is terminated after finishing the Kth shifting processing. To represent $\hat{S}_{physiology}(t)$, all of the output IMFs from EEMD will be selected. Thus, there is no time wasted on decomposing redundant IMFs.

For EKG, there are P, Q, R, S, and T in a pulse. The interval between two successive R is called R-R interval (RR). Fig. 6 shows the detrending process of $RR(t)$ using AA-EEMD with early termination scheme.

B. *Adaptive Aligned*

The value of f_{thr} determines the number of IMFs decomposed by EMD before early termination. K is varying for different physiological signals and different subjects with a fixed f_{thr}. Thus, determination of K is adaptive.

By setting a reasonable f_{thr}, the control block adaptively determines a K to avoid the interference of the trends and to interpret the physiological meaning of physiological signals. On the one hand, smaller f_{thr} leads to larger K, which infers that more IMFs will be summed for further MSE analysis. In addition to the IMFs related to physiological meanings, the IMFs arising from background signals will be involved. On the other hand, larger f_{thr} leads to smaller K, which infers that fewer IMFs will be summed for further MSE analysis. Some IMFs related to physiological meaning will be removed.

The value of f_{thr} is related to the signal which is analyzed. The following are the physiological meaning of EKG, ABP and PPG parameters in the high frequency (HF) range and low frequency (LF) range. Heart rate variability has a significant relation to autonomic nerve system. [10] defines the range of HF (0.15-0.4 Hz), LF (0.04-0.15 Hz), very low frequency (0.003-0.04 Hz) and ultra-low frequency (<0.003 Hz) power component. HF mainly reflects the vagal activity. LF mainly reflects sympathetic modulations or both sympathetic and vagal activity. In contrast, the physiological meaning of VLF and ULF are still unknown [11]. Pressure variability reflects the influence of respiration and the mechanisms of controlling the cardiovascular system. Pressure variability in frequency components is evaluated by the integration of the power in HF and LF range. Interaction of respiration and the thorax hemodynamic gives rise to HF, while the sympathetic modulations give rise to LF [12]. The variability of PPG can be applied to analyze autonomic function. The HF components reflect heart synchronous pulse waveform. The LF components reflect respiration, blood pressure control, thermoregulation and sympathetic nervous system activity [13-14].

By setting a reasonable f_{thr} for different physiological signals, the control block can adaptively determine a reasonable K when dealing with $\hat{S}_{measure}(t)$ from different subjects. For example, some $\hat{S}_{measure}(t)$ contain larger proportion of $\hat{S}_{trend}(t)$ than others. Thus, setting a fixed K for all $\hat{S}_{measure}(t)$ is improper. An adaptive mechanism for selecting K is necessary to unify the physiological meaning of MSE analysis.

IV. Experimental Data and Result

The experimental data came from intensive care unit (ICU) in National Taiwan University Hospital. EKG of the acute stroke patients was collected by the vital sign monitor. The simulations were done in MATLAB with a 4-core CPU.

The data collection number of EKG was 420. However, EKGs which were not collected within 24 hours after admission were not involved in our study as a research for early prediction of the acute stroke patients' functional outcome. Besides, EKGs which did not belong to stroke and those with poor signal quality were removed. At last, 224 acute stroke patients' EKGs remained in our analysis. Among these 224 stroke patients, 74 of them suffered from atrial fibrillation (AF), a kind of arrhythmia. The character of RR series of AF patients was similar to white noise [1]. Therefore, 224 acute stroke patients were further separated into two groups: 74 acute stroke patients with AF (AF stroke patients) and 150 acute stroke patients without AF (non-AF stroke patients). In this paper, we aim at 150 the non-AF stroke patients.

To evaluate the accuracy of our prediction, modified Rankin Scale (mRS) has been adopted. The mRS is a commonly used scale for measuring the degree of disability or dependence in the daily activities of stroke patients. The scale runs from 0-6, that is to say from no symptoms to death. In this paper, mRS 0-2 are grouped as good functional outcome, and mRS 3-6 are grouped as bad functional outcome. Table I is the summary of data collection.

MSE and T-MSE are applied to $RR(t)$. For each patient, the length of the input signals was 4000 points. The *SampEn* on each scale is higher in Fig. 7(b) than 7(a) mainly due to the removal of low-frequency trends. This phenomenon can be observed in the non-AF stroke patients both with good functional outcome and bad functional outcome. Compared to Fig. 7(b), the *SampEn* in 7(c) remains at small scale but obviously declines at large scale. This phenomenon can also be observed in the above groups. This is because when the f_{thr} becomes higher, more low-frequency components related to physiological signals are removed. Thus, there exists a trade-off. High f_{thr} thoroughly removes low-frequency trends, whereas low f_{thr} reserves low-frequency physiological information. To avoid the interference of the trends and to interpret the physiological meaning of physiological signals, f_{thr} is set to 0.01 Hz in our experiment.

It is worthwhile to note that the *SampEn* of the non-AF stroke patients with mRS 0-2 is higher than that of the non-AF stroke patients with mRS 3-6 on every scale. The area under the curve (AUC) of non-AF stroke patients with mRS 0-2 and

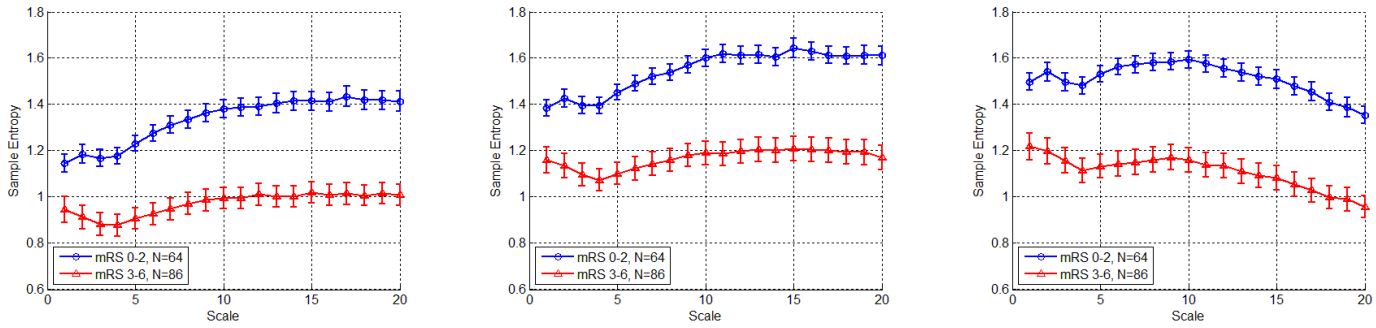

Fig. 7. Analysis result of EKG parameter—$RR(t)$. (a) MSE (b) T-MSE, whose f_{thr} is set to 0.01 Hz (c) T-MSE, whose f_{thr} is set to 0.02 Hz. The lateral axis is the scale factor τ, which runs from 0 to 20. The vertical axis is the *SampEn* for each scale. The stroke patients with good functional outcome (mRS0-2) and bad functional outcome (mRS3-6) are respectively represented by the blue line and red line. Values are expressed as mean ± standard error of the mean.

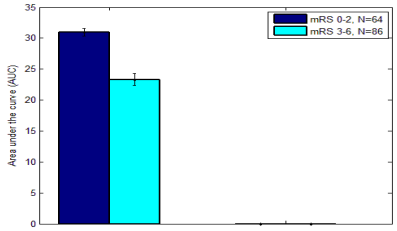

Fig. 8. The area under the curve (AUC) of non-AF stroke patients with mRS 0-2 and mRS 3-6. Values are expressed as mean ± standard error of the mean.

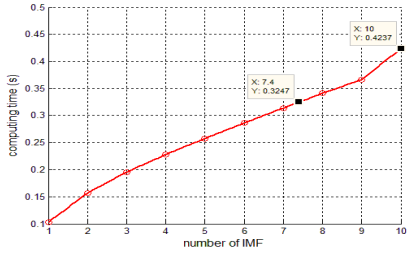

Fig. 9. The lateral axis is the number of IMF. The vertical axis is the average computing time of 150 non-AF stroke patients.

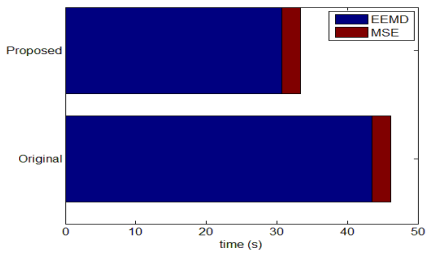

Fig. 10. Average computing time of original EEMD and MSE and proposed T-MSE based on AA-EEMD.

TABLE II. Summary of Experiment Result

Signal	Parameter	Average number of IMFs in a single member of ensemble			Average computing time in a single member of ensemble			Average computing time of combining EEMD and MSE			AUC (mean ± standard deviation)		
		Proposed AA-EEMD	Original EEMD	Pro. / Ori.	Proposed AA-EEMD	Original EEMD	Pro. / Ori.	Proposed T-MSE based on AA-EEMD	Original EEMD and MSE	Pro. / Ori.	mRS 0-2	mRS 3-6	*p*-value
EKG	$RR(t)$	7.4 IMFs	10.0 IMFs	74%	0.32 sec	0.42 sec	76%	33.3 sec	46.1 sec	72%	30.9 ± 5.2	23.3 ± 8.9	$8.93 * 10^{-9}$

mRS 3-6 is shown in Fig. 8. The result of one-way analysis of variance (ANOVA) in MATLAB shows significant statistical difference: $p = 8.93 * 10^{-9}$ while common significance level is $p = 0.05$.

AA-EEMD sets *K* adaptively when dealing with the signals measured from different subjects. Among 150 non-AF stroke patients, there are 124 patients whose $\hat{S}_{physiology}(t)$ is composed of 8 IMFs, and 60 patients whose $\hat{S}_{physiology}(t)$ is composed of 9 IMFs. This result reflects the necessity that *K* should be set adaptively instead of a fixed *K*.

Fig. 9 illustrates the importance of AA-EEMD in the perspective of number of decomposed IMFs and computing time. The original EEMD contain 10 shift processes and $\log_2(size)$ IMFs in a single EMD, where $xsize$ is the length of input. By using the original EEMD, the average number of IMFs decomposed from $\hat{S}_{measure}(t)$ is 10 IMFs, and the average computing time is 0.42 s. By using AA-EEMD, the average number of IMFs decomposed from $\hat{S}_{measure}(t)$ is reduced to 7.4 IMFs, and the average computing time is reduced to 0.32 s. That is, there are only 74.0% decomposed IMFs of the original and the computing time is reduced to 76.6%.

Fig. 10 shows the computing time of combining EEMD and MSE. As to original EEMD and MSE, the average computing time is 46.1 s. As to T-MSE based on AA-EEMD with early termination scheme, the average computing time is reduced to 33.3 s., that is to say 72% computing time of the original.

Table II summarizes the experiment results. The MSE result of EKG is consistent with the physiological control mechanism. The complexity of EKG is higher in the acute stroke patients with good functional outcome than those with bad functional outcome. In other words, AUC is larger in the acute stroke patients with good functional outcome than those with bad functional outcome. Therefore, AUC can be an index of predicting the acute stroke patients' functional outcome.

V. CONCLUSION

In this paper, we proposed a T-MSE based on AA-EEMD with early termination scheme. It can not only reduce the computing time, but also consider the frequency meaning of different physiological signals and different subjects. Furthermore, T-MSE based on AA-EEMD is applied to analyze the physiological signals of non-AF stroke patients in ICU. AUC is larger in the acute stroke patients with good functional outcome than those with bad functional outcome. For EKG parameter, the *p*-value of ANOVA is approximately 10^{-8}, which shows significant statistical difference. And the average number of IMFs in a single member of ensemble is reduced to 74% of the original. The average computing time in a single member of ensemble is reduced to 76%. Also, the average computing time of combining EEMD and MSE is reduced to 72%.

VI. REFERENCES

[1] M. Costa, A.L. Goldberger, and C.K. Peng,"Multiscale entropy analysis of biological signals," *Physical Rev. E*, vol. 71, no. 021906, pp. 1-18, Feb. 2005.

[2] P.H. Tsai, C. Lin, J. Tsao, P.F. Lin, P.C. Wang, N.E. Huang, et al., "Empirical mode decomposition based detrended sample entropy in electroencephalography for Alzheimer's disease," *Journal of neuroscience methods,* vol. 210, pp. 230-237, Sep. 2012.

[3] Z. Trunkvalterova, M. Javorka, I. Tonhajzerova, J. Javorkova, Z. Lazarova, K. Javorka, et al., "Reduced short-term complexity of heart rate and blood pressure dynamics in patients with diabetes mellitus type 1: multiscale entropy analysis," *Physiological Meas.*, vol.29, pp. 817-828, Jul.2008.

[4] C.W. Lu, M. Czosnyka, J.S. Shieh, A. Smielewska, J.D. Pickard, and P. Smieleswski,"Complexity of intracranial pressure correlates with outcome after traumatic brain injury," *Brain*, vol.135, pp. 2399-2408, Aug. 2012.

[5] M. Costa, A.L. Goldberger, and C.K. Peng, "Multiscale entropy analysis of complex physiologic time series," *Physical Rev. Lett.*, vol. 89, no. 068102, pp. 1-4, Aug. 2002.

[6] J.F. Valencia, A. Porta, M. Vallverdu, F. Claria, R. Baranowski, E. Orlowska-Baranowska, et al., "Refined multiscale entropy: Application to 24-h holter recordings of heart period variability in healthy and aortic stenosis subjects," *IEEE Transactions on Biomedical Engineering*, vol.56, no.9, pp.2202-2213, Sept. 2009.

[7] N.E. Huang, Z. Shen, S.R. Long, M.C. Wu, H.H. Shih, Q. Zheng, et al., "The empirical mode decomposition and the Hilbert spectrum for nonlinear and non-stationary time series analysis," in *Proc. R. Soc. Lond. A.*, vol. 454, no. 1971, pp. 903-995, Mar. 1998.

[8] X. Zhang, X. Chen, P.E. Barkhaus, and P. Zhou, "Multiscale Entropy Analysis of Different Spontaneous Motor Unit Discharge Patterns," *IEEE J. Biomed. Health Inf.*, vol.17, no.2, pp.470-476, Mar. 2013.

[9] W.C. Shen, Y.H. Chen, and A.Y. Wu, "Low-complexity sinusoidal-assisted EMD (SAEMD) algorithms for solving mode-mixing problems in HHT," *Digital Signal Processing*, vol. 24, pp. 170-186, Jan. 2014.

[10] D.P. Mandic, N. Rehman, Z. Wu, and N.E. Huang, "Empirical Mode Decomposition-Based Time-Frequency Analysis of Multivariate Signals: The Power of Adaptive Data Analysis," *IEEE Signal Process. Mag.*, vol.30, no.6, pp.74-86, Nov. 2013

[11] M. Malik, J.T. Bigger, A.J. Camm, R.E. Kleiger, A. Malliani, A.J. Moss, et al., "Heart rate variability standards of measurement, physiological interpretation, and clinical use," *European heart journal*, vol. 17, pp. 354-381, Mar. 1996.

[12] M. Di Rienzo, P. Castiglioni, and G. Parati, "Arterial blood pressure processing," in *Wiley Enciclopedia of Biomedical Engineering*, M. Akay, Ed. Hoboken, NJ: Wiley, 2006, pp. 98–109

[13] Korhonen, and A. Yli-Hankala, "Photoplethysmography and nociception," *Acta anaesthesiologica Scandinavica*, vol. 53, pp. 975-985, Sept. 2009.

[14] J. Allen, "Photoplethysmography and its application in clinical physiological measurement," *Physiol. Meas.*, vol. 28, pp. R1-R39, Mar. 2007.